PERGAMON

Water Research 37 (2003) 297–306

WATER RESEARCH

www.elsevier.com/locate/watres

Continuous-flow metal biosorption in a regenerable *Sargassum* column

B. Volesky[a,*], J. Weber[a], J.M. Park[b]

[a] *Department of Chemical Engineering, McGill University, 3610 University street, H3A 2B2 Montreal, Que., Canada H3A 2B2*
[b] *School of Environmental Engineering, Postech, Pohang, South Korea*

Received 12 February 2001; accepted 26 February 2001

Abstract

Metal biosorption behavior of raw seaweed *S. filipendula* in ten consecutive sorption–desorption cycles has been investigated in a packed-bed flow-through column during a continuous removal of copper from a 35 mg/L aqueous solution at pH 5. The elutant used was a 1% (w/v) $CaCl_2$/HCl-solution at pH 3. The sorption and desorption was carried out for an average of 85 and 15 h, respectively, representing more than 41 days of continuous use of the biosorbent. The weight loss of biomass after this time was 21.6%. The Cu-biosorption capacity of the biomass, based on the initial dry weight, remained relatively constant at approximately 38 mg Cu/g. Loss of sorption performance was indicated by a shortening breakthrough time and a broadening mass-transfer zone. The column service time, considered up to 1 mg Cu/L in the effluent, decreased continuously from 25.4 h for the first to 12.7 h for the last cycle. The critical bed length, representing the mass-transfer zone, increased almost linearly from 28 to 34 cm. "Life-factors" for *S. filipendula* were found to be 0.0008 h^{-1} for the breakthrough time and 0.008 cm/h for the critical bed length, using an exponential decay and linear fitting functions, respectively.

Regeneration with $CaCl_2$/HCl at pH 3 provided elution efficiencies up to 100%. Maximum concentration factors were determined to be in the range 16–44, a decreasing tendency was observed with an increasing exposure time.

Keywords: Column biosorption; Multi-cycle biosorption; Biosorbent regeneration; *Sargassum* biosorbent; Cu biosorption; copper removal

1. Introduction

Separation processes based on what is widely labeled as adsorption, followed by desorption are widely utilized. Due to its inherent effectiveness in an adsorption process the packed-bed reactor is generally preferred. Its advantage is the highest possible packing density of the sorbent, yielding a high volumetric productivity. The same configuration is to be used for metal biosorption processes based on novel biosorbent materials. With potentially enormous environmental applications in detoxification of metal-bearing industrial effluents, biosorption processes are considered as not only technically feasible but also economically very attractive.

The performance of packed-bed adsorbers is analyzed using the effluent concentration versus time curves. For adsorption the plot is usually referred to as the breakthrough curve, and for desorption it is the elution curve. Both curves are a function of the column flow parameters, sorption equilibrium and mass transport factors.

1.1. Definition of sorption column operating parameters

The breakthrough point is the time (t_b) when the sorbate appears in the effluent stream at some

*Corresponding author. Tel.: +1-514-398-4276; fax: +1-514-398-6678.
E-mail address: boya@chemeng.lan.mcgill.ca (B. Volesky).

0043-1354/02/$ - see front matter © 2002 Published by Elsevier Science Ltd.
PII: S0043-1354(02)00282-8

Nomenclature

b	Langmuir constant (L/mg, L/mmol)
c	metal concentration (mg/L)
c_i	initial or influent metal concentration (mg/L)
c_f	final metal concentration (mg/L)
c_e	effluent concentration (mg/L)
c_{tp}	maximum concentration for elution (mg/L)
$c_{1\,h,5\,h}$	concentration at 1 h resp. 5 h for elution (mg/L)
CFp	concentration factor considering maximum elution concentration (dimensionless)
$dc/dt_{i1,2}$	slope at first or second inflection point
D	axial dispersion coefficient (length^2/time)
E	elution efficiency (%)
F	flow rate (mL/min)
k_f	mass-transfer coefficient (length/time)
k_L	life-factor with respect to L_{min} (cm/h, cm/cycle number)
k_b	life-factor with respect to t_b (h^{-1}, (cycle number)$^{-1}$)
L_c	total length of column (cm)
L	length of packed bed (cm)
L_{min}	critical bed length (cm)
$L_{min,0}$	initial critical bed length (cm)
m_{ad}	metal mass adsorbed to the biomass (mg, g)
m_t	total metal mass run into the column (mg, g)
m_e	metal mass in effluent (mg, g)
m_d	metal mass desorbed (mg, g)
M	dry weight of biomass (mg, g)
$\Delta p_{b,e}$	pressure drop at beginning resp. ending for each regeneration cycle (kPa)
Pe	Peclet number (dimensionless)
q	metal uptake capacity of biosorbent (mg metal/g biomass)
q_{max}	maximum capacity of biosorbent (mg metal/g biomass)
S/L	solid-to-liquid-ratio (g biomass/mL solution)
t	time (min, h)
t_b	breakthrough point (h)
$t_{b,0}$	initial breakthrough point (h)
t_b^{eff}	effective breakthrough time (h)
t_e	exhausting time (h)
t_s	stoichiometric time (h)
$t_{1,2i}$	time of first or second inflection point (h)
t_p	time at concentration peak for elution (min)
Δt	mass-transfer zone (h)
$\Delta t/(2+t_b)$	half of the masss transfer zone referring to the whole time abscissa (h)
u	superficial velocity (cm/min)
U	fraction of used bed within the mass-transfer zone (%)
V	volume of metal solution (mL, L) total volume of column (mL) volume of packed bed (mL)
x	exposure time (h) cycle number
Δz	column section (length)

predetermined concentration. The time t_e is the time when the whole column sorption bed becomes totally saturated by the sorbate at its inflow concentration and the bed is no longer effective. The time interval between t_b and t_e corresponds to the length of the mass-transfer zone in the bed. The fact that real mass-transfer zones appear S-shaped in the plot is due to adsorption mechanism and mass transport conditions. These parameters are generally taken into consideration in deriving the column mass balance using the shell balance method [1]. For the differential column section Δz, the following differential equation describes the process:

$$-D_p\frac{\partial^2 c}{\partial z^2}+u_i\frac{\partial c}{\partial z}+\frac{\varphi_b}{\varepsilon}\frac{\partial q}{\partial t}+\frac{\partial c}{\partial t}=0. \quad (1)$$

The mechanism of the sorption process is reflected in the equilibrium isotherm. Rearranging Eq. (1) by neglecting axial dispersion shows the connection between the flow-through column mass-transfer zone and batch equilibrium data:

$$\frac{dz}{dt}=\frac{u_i}{1+\varphi_b/\varepsilon\partial q/\partial c}. \quad (2)$$

The term $\partial q/\partial c$, reflects the effect of adsorption mechanism. In the present case of biosorption, the Langmuir sorption isotherm applies and its derivatized form is

$$\frac{\partial q}{\partial c}=\frac{q_{max}1/b}{c^2+2c/b+1/b^2}. \quad (3)$$

While a high value of the maximum uptake capacity q_{max} and a high affinity, b, result in a desirable smaller mass-transfer zone, Eq. (3) hyperbolic function values decrease with increasing concentration. This causes the so-called "self-sharpening" effect of favorable isotherms on the breakthrough curve. At concentrations exceeding the favorable range (at q_{max}) the self-sharpening effect on the breakthrough curve is lower. In contrast, the Langmuir isotherm is nearly linear when operating at

very low concentrations, resulting in spreading of the breakthrough curve. The mass-transfer zone moves through the bed getting wider along the way.

Mass transfer considerations also tell us that the bigger the diameter of the particle (d_p), increasing the intraparticle diffusional resistance, the flatter the breakthrough curve [1]. It should be mentioned that the column inlet concentration has no influence on the breakthrough time t_b as long as the linear and favorable isotherm range is not exceeded since an increasing concentration results in an increasing capacity. In the present experiment, a feed concentration of $c_i = 35$ mg/L was used corresponding to a nearly linear equilibrium isotherm relationship where the self-sharpening effect was not expected.

The column feed flow rate affects not only the extraparticle mass transfer coefficient, but in particular, the overall sorption kinetics. The degree of flow dispersion in the sorption column is described by the dimensionless Peclet number [2]: both increasing with the column length.

The breakthrough and elution curves obtained in the present experiments need to be examined quantitatively. The quantity of metal retained in the column, represented by the area above the breakthrough $c-t$ curve, is obtained through integration carried out numerically in this work by using the computer program ORIGIN. Dividing the metal mass by the mass of the sorbent (M) leads to the uptake capacity q of the biosorbent. This corresponds to a point on the equilibrium isotherm, whereas the influent concentration in the column corresponds to the final equilibrium concentration (c_f).

The breakthrough point t_b was defined as the time when the effluent concentration of copper reached 1 mg Cu/L, which is the recommended limit for drinking water [3]. The bed exhaustion time t_e was selected as 34 mg Cu/L in the effluent. The time period from t_b to t_e ($= \Delta t$) is related to the length of the sorption zone. The metric length of this zone can be approximately calculated from the breakthrough curve by an equation suggested by Ruthven [4]:

$$L_m = L\left(1 - \frac{t_b}{t_e}\right), \tag{4}$$

where L is the total length of the sorption bed and L_m is the length of the adsorption zone, which is also called the minimum or critical bed length. This parameter reflects the shortest possible sorbent bed length needed to obtain the breakthrough time t_b at $t = 0$.

In order to analyze breakthrough curves, their geometry needs to be examined. A "normal" curve is S-shaped and symmetric. Then, the inflection point corresponds to half of the mass transfer zone ($\Delta t/2 + t_b$), where half of the influent concentration is found in the effluent. To obtain the inflection point for non-symmetric breakthrough curves, a polynomial regression was carried out from t_b to t_e. The regression function was differentiated, whereby the time at the maximum corresponds to the inflection point (time t_i). Usually, a polynomial regression of the third order is sufficiently accurate to fit an S-shaped curve, yielding correlation coefficients of at least 99.8%. For very irregular breakthrough curves, a polynomial regression of the fourth order was necessary. That leads to a second inflection point (time t_{i2}) and is obtained at the minimum after taking the derivative of the fitting function.

The elution curve obtained for a displacement desorption performed in the present work is usually shaped as an asymmetric frequency distribution curve, which had a sharp increase and a flatter decrease. First of all, the curve is examined with regard to the elution efficiency (E) that is calculated by integrating the elution curve. The area below the curve multiplied by the feed rate leads to the metal mass desorbed (m_d):

$$m_d = F \int c_e \, dt. \tag{5}$$

The ratio between m_d and the metal mass bound to the biomass from the previous sorption ($m_{biomass}$) is the elution efficiency. Furthermore, the time of the peak (t_p) and the maximum concentration (c_p) are of interest, whereby the latter divided by the metal influent concentration (35 mg/L) expresses the overall sorption process concentration factor CF.

2. Materials and methods

2.1. Biomass

The experiments in a continuous flow-through column were performed with native *S. filipendula*. Before packing, the raw biomass was washed twice with distilled water and dried in the oven (45°C). Subsequently, the biomass was packed in the column by rewetting it in tap water, and washed with tap water until the conductivity in the effluent was constant and equal to that of tap water. Another washing step was conducted with 1% $CaCl_2$ (w/v), dissolved in tap water and adjusted to pH 3 with 1 M HCl, until the calcium concentrations in the inlet and outlet were equal. The concentration of Ca was determined by the atomic absorption spectrometer (AAS) at $\lambda = 422.7$ nm. A technical grade of $CaCl_2$ was used (A&C American Chemicals).

2.2. Column

The column was a simple polyacrylic tube with an inner diameter (ID) = 2.5 cm, outer diameter (OD) = 3.13 cm, length (L_c) = 50 cm. At the top of the

column, an adjustable plunger was attached with a 20 μm selective filter of 1.1 mm thickness. There was a stainless sieve with a mesh size of 70 (0.5 mm) at the bottom of the column.

2.3. Sorption and desorption process

Thirty-eight grams of dry biomass was packed within the column yielding an initial height of 41 cm and a packing density of 189 g/L, with a column active volume of 0.201 L. A 3 cm high layer of glass beads (3 mm in diameter) was placed on top of the packed biosorbent for better flow distribution. A downflow sorption process used a solution of 35 mg/L copper (from $CuSO_4 \cdot 5H_2O$) prepared with tap water, pH 5 was adjusted by using 1 M HCl. The flow-rate 15 mL/min, corresponding to 3.05 mL/min cm^2 (expressed as superficial velocity in cm/min) was delivered by a peristaltic pump (Cole-Parmer model Masterflex) and controlled by a flow-meter (Dwyers) and an in-line flow-pulse dampener. A pressure gauge at the column inlet measured the pressure drop across the column. Column effluent samples were collected by a programmable fraction collector (Gilson, model FC205) and analyzed by the AAS. The pH of the influent and effluent was recorded. Fig. 1 illustrates the experimental arrangement.

The desorption process used a 1% $CaCl_2$ tap water solution (technical flakes) acidified to pH 3 with 1 M HCl. The flowrate was varied in some cases between 10 and 20 mL/min. To determine the weight loss after ten regeneration cycles, the biomass was washed with distilled water and dried in the oven at 45°C overnight.

3. Results

3.1. Multiple sorption–desorption cycles

Ten sorption and desorption cycles were carried out with a column packed with raw *S. filipendula* biomass. The packed bed contained seaweed fragments of approximately 1 mm diameter and bladders, leaves and complete branches with a length of up to 5 cm. A copper bearing feed solution of 35 mg/L ($CuSO_4$) with pH 5 at a flow rate of 15 mL/min (3.05 cm/min) was passed through the column. The sorption process was stopped after reaching 35 mg Cu/L in the effluent and the regeneration solution of $CaCl_2$ (pH 3) was then pumped through the bed. One example of the resulting breakthrough and elution curves obtained is presented in Fig. 2 (cycle #10). The flow rate for the elution was varied as indicated. Table 1 summarizes the breakthrough time t_b, exhaustion time t_e, column capacity q and the mass transfer parameter. Table 2 lists the column operating parameters such as time, concentration at the peak (t_p and c_p), and the maximum concentration factor CF for each elution curve. Concentrations at 1 and 5 h were selected to illustrate the tailing of the curves.

After the 10th cycle the biomass was weighed. From the initial 38 g of raw *S. filipendula,* 29.8 g remained, with a weight loss of 21.6%. The length of the packed bed after the 10th desorption decreased from 41 to 38.5 cm. The bed volume and packed-bed density decreased accordingly. The volume became 6% smaller, from 201 to 189 mL. The resulting packed-bed density decreased from 189 to 158 g/L (16% less).

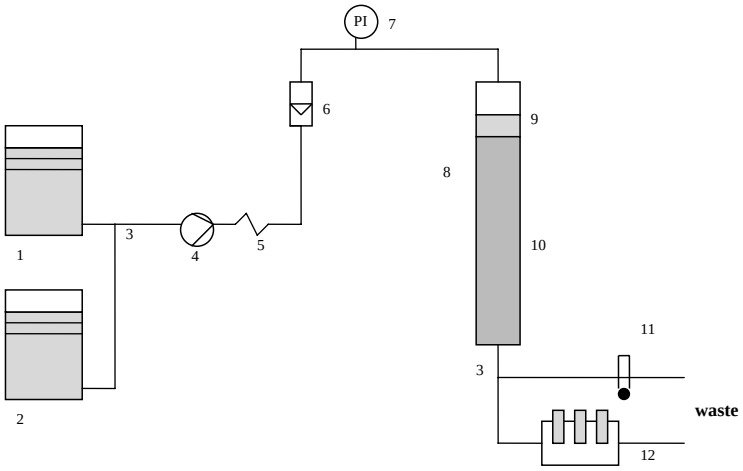

Fig. 1. Experimental arrangement for operating the biosorption packed-bed column: (1) stock container with $CuSO_4$-solution (20L), (2) stock container with $CaCl_2$-solution (20L), (3) three-way-valve, (4) peristaltic pump, (5) pulse dampener, (6) flowmeter, (7) pressure gauge, (8) column, (9) glass beads, (10) packed biosorbent, (11) pH measurement, (12) fraction collector.

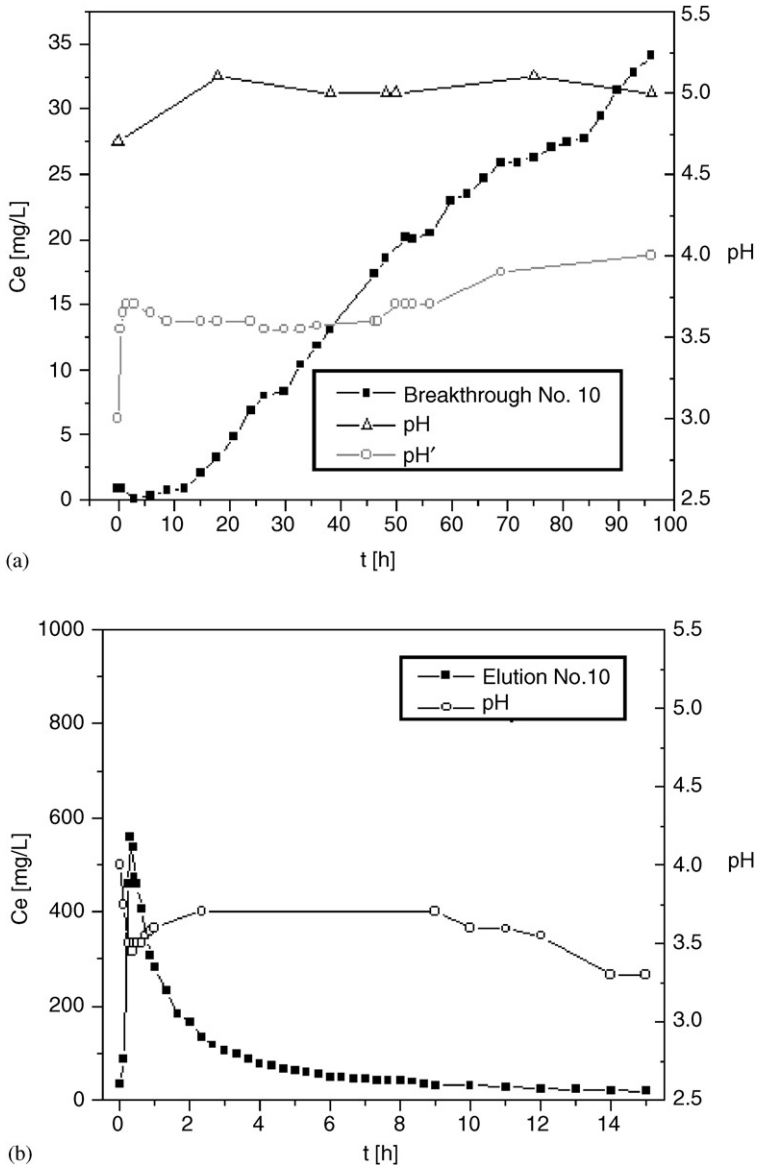

Fig. 2. *Sargassum filipendula* biosorption column performance in Cycle #10: column exit Cu concentration (■); (△) feed pH; (○) exit pH. (a) Breakthrough #10 characteristics of a column fed with Cu solution: Cu feed concentration $C_i = 35$ mg Cu/L at the superficial feed velocity 3.05 cm/min. (b) Elution #10 concentration profile for the Cu-saturated column desorption by $CaCl_2$.

3.2. Column sorption performance

The column breakthrough time t_b decreased from 25.4 h in the first cycle to 12.7 h in the tenth, the last one. Up to cycle 5, the decrease occurred in approximately 2 h steps. Afterwards, the decrease was more gradual. In the 6th and 7th cycles, the wash limit of 1 mg Cu/L could not be attained and an alternative value of 1.5 ppm was chosen instead for calculating the relevant mass transfer parameters.

The column was not washed after each elution operation. Instead, full-strength (35 mg Cu/L) feeding was immediately initiated. The effective breakthrough times t_b^{eff} for each uptake cycle are given in Table 1. This time indicates the real period of time when the concentration was below the breakpoint concentration. It is referred to as the transition between the desorption and sorption processes. Switching from the elution solution to the metal solution resulted in breakthrough concentration attainment with a delay. In order to

Table 1
Breakthrough parameters for ten sorption–desorption cycles

Break-through no.	q (mg Cu/g biomass)	t_b (h)	t_b^{eff} (h)	t_e (h)	Δt (h)	$\Delta t/2 + t_b$ (h)	t_s (h)	U (%)	t_{i1} (h)	dc/dt_{i1} (mg/L h)	t_{i2} (h)	dc/dt_{i2} (mg/L h)	L^b (cm)	L_{min} (cm)	Δp_b (kPa)	Δp_e (kPa)
1	38.2	25.4	25.4	79.5	54.1	52.5	46.5	39	38.5	1.10	67.9	0.21	41	27.9	13.3	20.6
2	37.0	23.1	22.3	77.0	53.9	50.05	45.0	41	36.1	1.11	65.1	0.13	41	28.7	19.3	26.0
3	34.7	21.2	20.4	62.0	40.8	41.6	42.5	51	40.2	0.97	—	—	40.5	26.7	20.7	20.7
4	38.2	18.5	17.7	67.7	49.2	43.1	44.0	52	34.4	0.95	62.1	0.39	40	29.1	26.7	33.3
5	34.3	17.0	16.2	69.0	52.0	43.0	42.0	48	37.0	0.77	—	—	40	30.1	28.7	33.3
6	37.7	10.0[a]	9.2	70.5	60.5	40.25	47.0	62	32.6	0.77	64.8	0.36	40	34.2	33.3	35.3
7	34.6	14.0[a]	13.2	69.5	55.5	41.75	42.5	51	35.6	0.93	69.0	0.15	40	31.9	27.3	20.0
8	32.2	14.0	8.0	72.5	58.5	43.25	39.5	44	43.0	0.82	65.0	0.18	40	32.3	20.0	20.0
9	36.1	14.5	13.7	81.0	66.5	47.5	50.5	53	34.4	0.56	60.8	0.39	40	32.8	20.0	20.0
10	42.4	12.7	12.7	95.3	82.8	54.1	54.0	50	31.9	0.54	73.2	0.23	39.5	34.2	20.7	23.3

[a] Break point limit of 1ppm not reached, for further calculation an alternative limit of 1.5ppm was set.
[b] Effective length, including interstices.

Table 2
Regeneration parameters for ten sorption–desorption cycles

Elution no.	F (mL/min)	Time of elution (h)	E (%)	t_p (min)	c_{tp} (mg/L)	CF_p	$c_{1\,h}$ (mg/L)	$c_{5\,h}$ (mg/L)	Δp_b (kPa)	Δp_e (kPa)
1	15	15	100.2	19.8	914.5	26.1	554.0	130	20.6	19.3
2	20	15	98.5	21.6	1542	44.1	256.2	47.7	33.3	32.0
3	10	15	92.5	35.0	1107	31.6	764.4	402.2	12.6	12.6
4	15	15	96.1	27.0	892	25.5	475.5	125.9	33.3	33.3
5	20	8	95.6	22.5	783	22.4	329.0	64.5	40.0	36.7
6	20	15	98.2	19.8	700	20.0	290.0	62.0	35.3	33.3
7	20	22	121.6	22.5	740	21.1	345.0	61.5	30.0	28.6
8	20	15	102.2	22.5	629	18.0	295.0	59.0	30.0	28.6
9[a]	20/15/15	15/1/15	102.9/104.9/105.4	22.0	623	17.8	338.5	52.5	30.0	30.0/20/20
10	20	15	91.0	19.0	557.5	15.9	282.2	62.5	36.0	38.6

[a] After 15 h $CaCl_2$ regeneration, 1 h HCl wash, followed by again 15 h $CaCl_2$ regeneration.

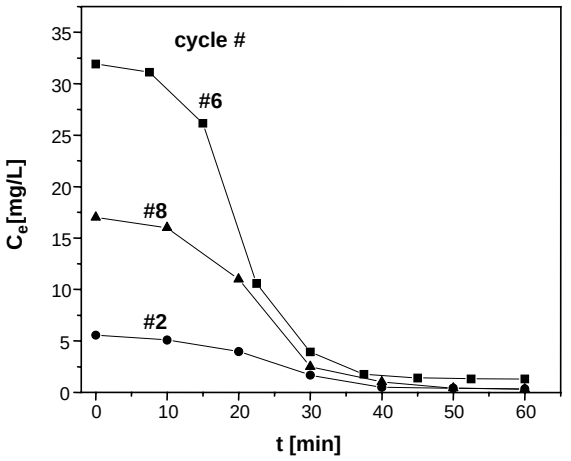

Fig. 3. Transition profile between desorption and sorption cycle obtained by enlargement of the breakthrough curves no. 2 (●), 6 (■), and 8 (▲) at the initial area. The previous elution time was 15, 8 and 22 h, respectively.

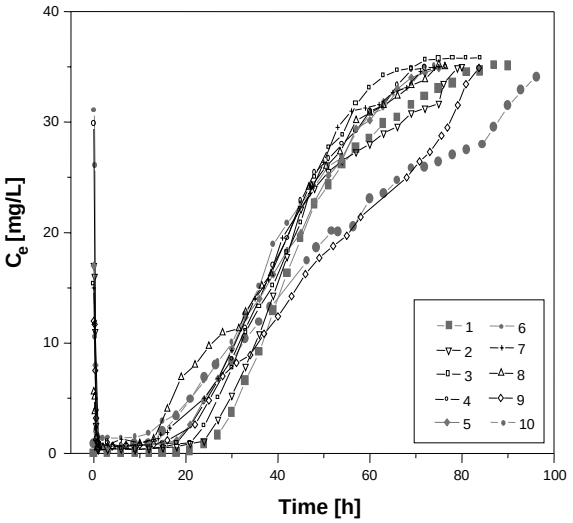

Fig. 4. Breakthrough curves for all 10 biosorption cycles.

obtain t_b^{eff}, this delay (t_d) had to be subtracted from the breakthrough time t_b. Fig. 3 contains enlargements of breakthrough curves no. 2, 6 and 8 to determine t_d for different concentrations. The resulting $t_d \sim 45$ min (~ 0.8 h) was independent of the concentration in that range.

The biosorption column capacity, related to the initial dry weight of biomass (38 g) loaded in, shows no correlation with the decreasing breakthrough time. The copper uptake obtained in the first sorption cycle (38.2 mg Cu/g) corresponds nearly exactly to the uptake obtained from the sorption isotherm (38.5 mg Cu/g) at the equilibrium concentration of 35 mg/L [5] with no decreasing tendency in the following cycles. In the last cycle the initial column capacity was even exceeded (at 42.4 mg Cu/g) probably due to the previous more thorough desorption ($CaCl_2$ wash, HCl wash and $CaCl_2$ regeneration).

A decreasing breakthrough time and approximately steady capacity are proven by an increasing length of the mass transfer zone and a decreasing slope at the (first) breakthrough inflection point. The mass transfer zone is described by the difference between the breakthrough and the exhaustion time (Δt), and by the critical bed length L_{min}. Comparing the first and the last cycles, Δt differs by 53% (28.7 h), whereas the difference in terms of L_{min}amounted to only 22.6% (6.3 cm). Δt reflects the overall sorption zone, whereas the critical bed length is perhaps a more appropriate parameter for evaluation of the mass transfer zone in terms of the current length of the packed bed (Eq. (5)).

The actual length of the bed was not constant during the ten experimental cycles. On the one hand, the total length of the bed decreased, but also hollow spaces up to 1 cm length appeared within the bed. To consider both, the current length is indicated as an effective one (see Table 1). While the initial bed length was 41 cm, eventually decreasing to 39.5 cm, the transfer zone length increased with the increasing cycle number—both lengths come generally closer to each other.

The slopes of subsequent breakthrough curves do not flatten considerably up to the 8th cycle after which they decreased sharply. The slope in the last cycle (0.54 mg/L h) was only half that of the first cycle (1.1 mg/L h) as is clearly seen in Fig. 4 where all breakthrough curves are plotted in one diagram.

3.3. Biosorption column life-factors

The rate of decreasing sorption performance can be evaluated following the concept of deactivation of heterogeneous catalysts [2]. For biosorption, the activity-indicator can be calculated as "life-factors" based on the breakthrough time, bed sorption capacity and/or critical bed length illustrated in Fig. 5 with regard to the number of cycles and exposure time (calendar life, including the sorption and desorption time).

For calculating the life-factor in terms of the critical bed length, a linear regression gave the best fit for the data points, the slope representing the life-factor k_L:

$$L_{min} = L_{min,0} + k_L x, \quad (6)$$

where x represents the cycle number or exposure time, $L_{min,0}$ the initial critical bed length.

For $L_{min,0}$, a value of 26.6 cm was determined, giving $k_L = 0.008$ and 0.8 cm/cycle. The correlation coefficient r was 86.9% which could be 98.7% if cycles #3 and #6

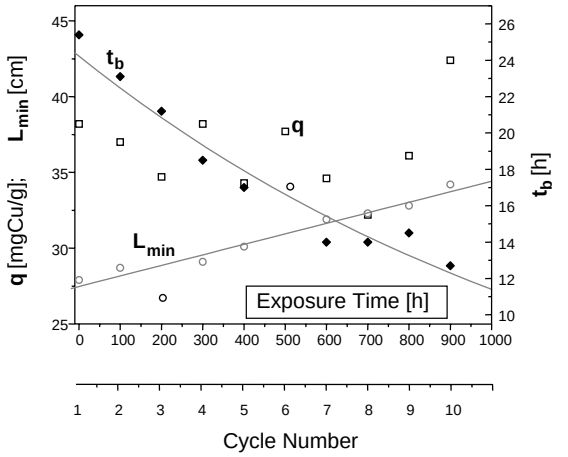

Fig. 5. The sorption column capacity q (□), the critical bed length L_{min} (○) and the breakthrough time t_b (♦) with respect to the sorption contact (exposure) time and the cycle number. For the critical length and the breakthrough time "life-factors" can be calculated from a linear and an exponential decay fitting function, respectively.

data points were regarded as anomalies (k_L would be 0.007 and 0.7 cm/cycle).

For the breakthrough time an exponential decay function regression was chosen:

$$t_b = t_{b,0} \exp(-k_b x), \quad (7)$$

where $t_{b,0}$ is the initial breakthrough time and k_b the corresponding life-factor. The data point from sorption cycle #6 was omitted because of the anomalous preceding insufficient elution. $t_{b,0} = 24.7$ h was determined, giving the life-factor $k_b = -0.0008\,h^{-1}$ and $-0.08\,(cycle)^{-1}$. A determination of the life-factor for the biosorbent capacity was not carried out since no decreasing tendency could be recognized.

3.4. Geometry of breakthrough curves

While the early cycle breakthrough curves showed relatively uniform shapes, slightly flatter profiles could be noticed after cycle 6. The geometry of the breakthrough curve is described by the stoichiometric time and the time at the inflection point which for a symmetric curve become identical at half of the mass transfer zone, represented by $\Delta t/(2 + t_b)$ in Table 1. All the mass transfer describing time parameters [$\Delta t/(2 + t_b)$, t_s and t_i,] come close together and the mass transfer zone appeared the shortest for sorption cycle #3.

The symmetry of a curve is readily seen as the fraction of used bed in the mass transfer zone (U). This parameter is based on the same principle as the stoichiometric time. While for a symmetric breakthrough curve this value is 50%, the biggest deviations from 50% can be observed in cycles #1 and #6 with values of 39% and 62%, respectively.

3.5. Elution

In repeated sorption–desorption cycles, the sorption performance is necessarily related to the preceding cycle desorption efficiency which was always at least 95% in this experimental series. An exception was desorption #3 which was carried out at 10 mL/min (2.04 cm/min), desorbing only 91.5% of copper. The desorption was usually conducted in 15 h cycles, resulting in residual effluent concentrations between 12 and 17 mg Cu/L. After a shorter (8 h) cycle #5 (95% elution efficiency), the metal concentration at the end of elution, was 32 mg Cu/L (see Fig. 3 and the subsequent sorption cycle #6 could not reach the breakthrough point of 1 ppm. A longer desorption (22 h) in cycle #7 yielded 121% metal release flushing out the leftover metal as confirmed by back-calculating the copper mass balances.

The desorption efficiency was flow-rate dependent. Elution curves show desirably small tailing at 20 mL/min (4.07 cm/min), as seen by the $c_{1\,h}$ and $c_{5\,h}$ values. $c_{5\,h}$ averaged 58.5 h at 20 mL/min which is half of the $c_{5\,h} = 128$ h at 15 mL/min, and 1/6 of $c_{5\,h}$ at 10 mL/min (402 h). At 20 mL/min the maximum concentration was also reached in a shorter time $t_p = 20$ min ($t_p = 23$ and 35 min for 15 and 10 mL/min, respectively). However, the maximum concentration and the corresponding concentration factor, did not correlate with the desorption performance and flow rate. The highest peak of 1542 mg Cu/L for the elution part of cycle #2 at 20 mL/min was not reached again even approximately.

When the elution efficiency was related to the flow rate, it could be seen that for the same elution time at 20 mL/min, 50% and 75% of the elution volume was used at 10 and 15 mL/min, respective flow-rates.

3.6. Effluent pH and column pressure drop

The effluent pH, illustrated in Fig. 2 for all the process cycles, describes the course of the breakthrough in a qualitative way. For each cycle, after a short increase, the pH decreased until the breakthrough which occurred at approximately 20 h. Then, the pH increased as the saturation of the bed progressed. The feed pH 5 was not reached in any cycle at the end of the sorption process. At the end of the breakthrough, the pH ranged from 4 to 4.4 for all cycles, while the pH peak at the beginning was between pH 3.5 and 5.3, depending on the previous desorption. The elution pH profile was similar for all regeneration cycles, nearly mirroring the elution curve shape.

Tables 1 and 2 also present the pressure drop (Δp) across the column at the beginning and at the end of each cycle reflecting changes in the bed structure. Hollow spaces and bubbles occurred within the column, low-temperature tap-water carbonate likely contributing to the bubble development. The column pressure drop appeared to correlate with the bubble presence.

4. Discussion

Biosorption performance of biomass of brown marine alga *S. filipendula* was investigated in multiple sorption/regeneration cycles. Together with equilibrium biosorption capacity and rate data, the "life-factors" information is useful for the design of a regenerative sorption system. Due to difficulties with producing biosorbents in suitable particles, most of earlier regeneration studies were conducted in batch equilibrium systems or were restricted to a few cycles. Acid elution (HCl) has been succesful, causing no decrease in Cd uptake for crosslinked *S. fluitans* [6] and crosslinked *Ascophyllum nodosum* [7]. The cobalt uptake of not crosslinked *A. nodosum*, however, decreased severely after acidic desorption [8].

More "realistic" process conditions used in the present study included the use of raw biomass, industrial-grade chemicals ($CaCl_2$) and tap water. While a constantly shortening breakthrough time from cycle to cycle was observed, the uptake capacity exhibited no decreasing trend. The mass transfer sorption zone broadened with increasing "age" of the biosorbent. A significantly flattened overall adsorption zone Δt, however, could only be noticed for the last two of the 10 sorption runs (Fig. 4). The reason for the shortening breakthrough time was apparently not the diminishing equilibrium uptake capacity, but rather a slight change in the column overall adsorption rate. That means that while sorbing sites of the biomass were still available, they became less accessible.

A loss of sorption performance during the long-term use may have a variety of reasons. It may be caused by changes of the chemistry and of the structure of the biosorbent, as well as by changes of the flow and mass transport conditions within the column. Deteriorating sorption properties may be due to chemical changes of the cell wall components such as alginate and sulfated polysaccharides which play a major role in biosorption by marine algae [9]. Trace contaminants in the tap water and in the $CaCl_2$ regenerating solution may accumulate on the biomass and block the binding sites or affect the stability of these molecules.

While there was some biomass weight loss over the 10 process cycles, the uptake, based on the final biomass weight even increased: 54 mg Cu/g biomass instead of 42.4 mg Cu/g biomass. The uptake capacity in Table 1 has to be regarded as an "effective" one since it is related to the initial weight of biomass. In the last cycle, the uptake capacity was enhanced by an acidic elution, just as noted earlier [6]. In general, a shortened breakthrough time and a broadened mass transfer zone are usually caused by an unequal packed-bed density and unequal flow patterns within the column. Both could easily be blamed for the irregularities in the present work where the biomass apparently moved in the bed and lost some mass.

The use of only one wash step was the aim for regenerating the biosorbent in this work. That could be achieved with a $CaCl_2$/HCl mixture at pH 3. The use of a better pure HCl elutant would eventually call for another washing step to adjust the pH within the column and appropriately regenerate the biosorbent. Higher desorption flow rates resulted in the desirable smaller tailing of the elution curve and the maximum concentration was reached in a shorter time. The maximum metal concentration in the elutant, however, showed no clear correlation with the flow rate. In order to assure the regeneration capability and elution efficiency in one process, the desorption would have to be optimized.

Effluent pH variations correspond to the breakthrough and elution course and can be useful for a simplified control of a column biosorption process. In general, regenerative biosorption system with *S. filipendula,* or another *Sargassum* biosorbent, appears feasible under relatively simple conditions adopted in the present work.

References

[1] Hines AL, Maddox RN. Mass transfer, fundamentals and application. Englewood Cliffs, NJ: Prentice-Hall, 1985. p. 456–93.

[2] Levenspiel O. Chemical reaction engineering. New York, NY: Wiley, 1962, p. 242–308.

[3] Corbitt RA. Standard handbook of environmental engineering. New York, NY: McGraw-Hill, Inc, 1989, Chap. 5.14.

[4] Ruthven DM. Principles of adsorption and adsorption processes. New York: Wiley, 1984, p. 86–123, 278–9, 124–282.

[5] Volesky B, Weber J, Vieira RHSF. Biosorption of Cd and Cu by different types of *Sargassum* biomass. In: Amils R, Ballester A, editors. Biohydrometallurgy and the Environment Toward the Mining of the 21st century (Part B): International Biohydrometallurgy Symposium—Proceedings. Amsterdam, The Netherlands: Elsevier, 1999. p. 473–82.

[6] Aldor I, Fourest E, Volesky B. Desorption of cadmium from algal biosorbent. Can J Chem Eng 1995;73: 516–22.
[7] Holan ZR, Volesky B, Prasetyo I. Biosorption of cadmium by biomass of marine algae. Biotechnol Bioeng 1993;41:819–25.
[8] Kuyucak N, Volesky B. Desorption of cobalt-laden algal biosorbent. Biotechnol Bioeng 1989;33:815–22.
[9] Fourest E, Volesky B. Contribution of sulphonate groups and alginate to heavy metal biosorption by the dry biomass of Sargassum fluitans. Environ Sci Technol 1996;30:277–82.